Cascade and dynamo action in a shell model of magnetohydrodynamic turbulence

Peter Frick
Institute of Continuous Media Mechanics, Korolyov 1, 614061 Perm, Russia

Dmitriy Sokoloff
Department of Physics, Moscow State University, 119899 Moscow, Russia

(Received 27 June 1997)

A shell model of magnetohydrodynamic turbulence, which allows one to conserve all the integrals of motion in both two and three dimensions, is proposed and studied. We demonstrate that this model reproduces basic facts known in the small-scale turbulent dynamo theory. In particular, we consider a process of redistribution of magnetic helicity generated by the mean-field dynamo, described in the model as magnetic forcing, into a small-scale magnetic field. We argue that the resulting equilibrium magnetic field spectrum strongly depends on the level of magnetic helicity and cross helicity, introduced by the large scales. The spectra with spectral index ''$-5/3$'' dominate if the cross helicity vanishes. If the level of cross helicity is high (correlated velocity and magnetic field) the spectra depend on the magnetic helicity: the strong magnetic helicity suppresses any cascade providing steep spectra, while the vanishing helicity of turbulent magnetic fields results in the occurrence of Kraichnan-Iroshnikov spectral index ''$-3/2$.'' [S1063-651X(98)04103-8]

PACS number(s): 47.27.Gs, 47.27.Eq, 47.65.+a, 91.25.Cw

I. INTRODUCTION

A turbulent flow of electrically conductive fluid can in principle generate magnetic field in two different ways. The most well known is a generation of large-scale magnetic field under the actions of helicity and, possibly, differential rotation in a rotating body with a turbulent flow without reflection symmetry (see, e.g., Moffatt [1]). This self-exciting large-scale magnetic field being affected by turbulent velocity field also gives rise to small-scale magnetic fields, which play an important role in this dynamo process. However, it is also possible to excite small-scale magnetic fields by a turbulent flow, which is statistically symmetric in reflection. This process was suggested by Batchelor [2]. A quantitative description of a small-scale dynamo was given by Kazantsev [3] and Kraichnan and Nagarajan [4] and developed by Vainstein [5,6]. A kinematic model of turbulent dynamo considered by Kazantsev [3] is based on a short−correlated velocity field and has been thoroughly investigated by numerical and analytical methods (see, e.g., Novikov *et al.* [7], Zeldovich *et al.* [8]). Some more realistic models of turbulent dynamo have been investigated numerically (e.g., Meneguzzi *et al.* [9]).

Based on these studies the main properties of the turbulent dynamo can be summarized as follows. The growth rate of magnetic field is estimated as v/l, where v is a turbulent velocity scale and l is a turbulent spatial scale. Self-exciting turbulent magnetic fields are expected to be very intermittent, organized in thin ropes, with the length of order l and the thickness of the order of dissipative scale of magnetic field. A nonlinear stabilization of magnetic field growth is likely to occur on the level of equipartition with kinetic energy.

However, the general situation with the turbulent dynamo is far from being completely understood. The turbulent dynamo properties can be model dependent, e.g., an acoustic wave turbulent generates magnetic field much worse than a vortex short-correlated velocity field [10].

The spectral properties of turbulent magnetic fields are also not very clear. Kinematic models of magnetic field generation give a quite unusual spectrum, growing with wave vector k and reaching the maximum near the dissipation scale. Conventional considerations lead to the conclusion that a nonlinear regime should result in a spectrum that decays with k and maximal near l (see, e.g., Ruzmaikin and Shukurov [11]). A quantitative description of this change in spectral properties was suggested by Kulsrud and Anderson [12]. For small-scale magnetohydrodynamic (MHD) turbulence, which develops under a strong large-scale magnetic field, a dimensional analysis predicts a $k^{-3/2}$ power law (Iroshnikov [13], Kraichnan [14]).

Possibilities of direct computer simulation, not to mention analytical methods, are very restricted in the case of nonlinear turbulent phenomena at large magnetic Reynolds numbers. Therefore any reasonable simplification of corresponding equations seems to be very attractive. Below we develop a description of a turbulent dynamo process in terms of a shell cascade model. The basic idea of these models is to represent each spectral range of a turbulent velocity and magnetic field with a few variables and to describe magnetic and kinetic energy evolution in terms of relatively simple ordinary differential equations, ignoring details of its spatial distributions. In spite of the obvious fact that shell models give only a simplified description of turbulence, they appear to be a reasonable tool in turbulent studies. In a certain sense, consideration of the turbulent dynamo in terms of shell models can be supplemented by consideration of cellular models [15,16] and closure methods of dynamo in maps [17] (see for review Childress and Gilbert [18]). These methods focus attention on the spatial magnetic field distribution rather than on the complicated hierarchical structure of velocity field.

A number of shell models for MHD turbulence were proposed (Frick [19], Gloaguen *et al.* [20], Grappin *et al.* [21], Carbone [22], Brandenburg *et al.* [23], Biskamp [24]) to

verify its spectral properties. These models involved free parameters and conserved only two invariants. Based on these models the authors demonstrated the difference between the hydrodynamical and magnetohydrodynamical turbulence [19–21], and studied the parameters of intermittency [22]. However, none of these models was capable of giving a stable solution, such as Kraichnan-Iroshnikov's law, for a stationary forced case. Biskamp obtained a solution close to $k^{-3/2}$ by introducing an additional interaction of any variable with the large-scale magnetic mode B_0.

Recently, an integral of motion, which, in a sense, is similar to helicity has been discovered for a class of hydrodynamic shell models [25]. We generalize this idea to a shell model relevant for a turbulent dynamo and consider a model, that enables one to conserve all the integrals of motion known for MHD in two-dimensional (2D) and 3D cases, respectively. Our main aim is to investigate the properties of growing solution and to investigate the spectral properties of stationary forced turbulence depending on the level of the magnetic helicity and the cross helicity, which are introduced in the small scales by the large-scale MHD flow.

Generation of a turbulent magnetic field is a specific 3D phenomenon; according to Zeldovich's theorem [26] an unbounded growth of magnetic field in 2D flow is impossible. In the present paper, we demonstrate that this result is well described by the shell model under consideration and compare the results for 2D and 3D cases. The essential difference between 2D and 3D cases with respect to the turbulent dynamo can be presented as follows. The first phase of magnetic field generation, i.e., stretching of a magnetic loop by a turbulent flow, is possible both in 3D and in 2D. In the latter case this results in a temporary magnetic energy growth. However, a magnetic loop in 2D is closed or almost closed. During the stretching process some sections of the tube with an oppositely directed magnetic field meet, which leads to a local cancellation of magnetic field (see [27]). This cancellation results in final magnetic field decay. In contrast, a twisting and folding of 3D magnetic line results in a magnetic field growth.

Dynamo effects have been already studied in terms of MHD shell models. More than 10 years ago Gloaguen *et al.* [20] studied a simple shell model, mainly concentrating on the dynamo effect. Frick [19] in his analysis of a shell model for 2D MHD turbulence showed that the Zeldovich antidynamo theorem holds true. However, it was still unclear whether these fine properties of turbulence can be reproduced by a simple shell model, in which the spatial dimension (2D or 3D cases) is described only in terms of conservation laws.

In this paper, we also demonstrate the role of quadratic invariants of motion (which are determined by 2D or 3D conservation laws) in a stationary forced MHD turbulence. We show that control over the injection of these quantities by external forces results in a corresponding change in spectral properties of small-scale MHD turbulence.

The outline of the paper is as follows. After a brief summary of the so-called Gledzer-Ohkitani-Yamada shell model, we introduce in Sec. II a shell model for MHD turbulence. Numerical study of free-decaying 2D and 3D MHD turbulence is described in Sec. III A, the dependence of spectral laws in inertial range upon the forcing is shown in Sec. III B. The discussion of the results is provided in Sec. IV.

II. SHELL MODEL

A. Gledzer-Ohkitani-Yamada shell model for HD turbulence

The shell models were introduced in the 1970s [29,28] as an attempt to mimic the Navier-Stokes equations via dynamical systems with limited degrees of freedom. They are constructed by truncations of the Navier-Stokes equations in the Fourier space, retaining only one real or complex mode U_n as a representative of all the modes in the shell with a wave number k ranging between $k_n=k_0\lambda^n$ and $k_{n+1}=k_0\lambda^{n+1}$. The parameter λ characterizes the ratio between two adjacent scales. It is one of the parameters of the model, and is usually taken equal to $\lambda=2$ (then every shell corresponds to an octave of wave numbers). Hereafter, we shall use this value. The coupling between the shells is chosen such as to preserve the main symmetries and properties of the Navier-Stokes equations. In this paper, we take for a basis the so-called GOY shell model (Gledzer [28], Ohkitani and Yamada [31]) in the form introduced in [30], which is governed by the following set of complex ordinary differential equations:

$$(d_t+\nu k_n^2)U_n=ik_n\left\{U_{n+1}^*U_{n+2}^*-\frac{\varepsilon}{2}U_{n-1}^*U_{n+1}^*-\frac{(1-\varepsilon)}{4}U_{n-2}^*U_{n-1}^*\right\}+f_n. \tag{1}$$

Here, $*$ stands for the conjugate, f_n is a random force, acting only on the few shells near $n=0$, and ε is a free parameter. Equation (1) gives the model of Gledzer [28] if $\varepsilon=5/4$ and the model of Ohkitani and Yamada [31] if $\varepsilon=1/2$. The properties of this model for different values of ε were investigated by Biferale *et al.* [30] and Frick *et al.* [32]. In a fully developed turbulence, an important dynamical quantity is the spectral flux of energy. The corresponding quantity in the shell models is the flux of energy Π_n from shells with $k<k_n$ to shells with $k\geqslant k_n$, which can be written as

$$\Pi_n=\left\langle \mathrm{Im}\left[k_nU_nU_{n-1}\left(-\frac{1}{2}U_{n+1}+\frac{\varepsilon-1}{4}U_{n-2}\right)\right]\right\rangle, \tag{2}$$

where $\langle\ \rangle$ denotes the time averaging. The GOY class of shell models is also characterized by a number of conservation laws, in the inviscid, force-free limit. The conserved quantity W can be written as

$$W=\sum_n |U_n|^2z^n, \tag{3}$$

where z satisfies the quadratic equation [25]

$$(\varepsilon-1)z^2-\varepsilon z+1=0. \tag{4}$$

This equation admits two solutions, $z=1$ and $z=1/(\varepsilon-1)$. The first solution corresponds to the energy conservation:

$$E=\sum_n |U_n|^2, \tag{5}$$

which is a conserved quantity common to all shell models (for any ε). The second solution corresponds to the conservation of a quantity

$$H=\sum_n\ [\mathrm{sgn}(\varepsilon-1)]^n k_n^{\alpha}(\varepsilon)|U_n|^2, \tag{6}$$

where $\alpha(\varepsilon)=-\log_2(|\varepsilon-1|/2)$. Here one can differentiate between two cases. If $\varepsilon>1$, the conservation value of H is a positively defined value, like generalized enstrophy, because $\mathrm{sgn}(\varepsilon-1)=1$. However, if $\varepsilon<1$, then $\mathrm{sgn}(\varepsilon-1)=-1$ and the value of H can be negative as well as positive. In this case, Kadanoff *et al.* [25] consider H as an analog of helicity.

B. Shell model for MHD turbulence

The MHD equations, written for the velocity $\vec{u}$ and the magnetic field $\vec{B}$ in the dimensionless form, are

$$\partial_t\vec{u}+(\vec{u}\cdot\vec{\nabla})\vec{u}=(\vec{B}\cdot\vec{\nabla})\vec{B}-\vec{\nabla}\left(P+\frac{B^2}{2}\right)+\mathrm{Re}^{-1}\Delta\vec{u},$$

$$\partial_t\vec{B}+(\vec{u}\cdot\vec{\nabla})\vec{B}=(\vec{B}\cdot\vec{\nabla})\vec{u}+\mathrm{Rm}^{-1}\Delta\vec{B},$$

$$\vec{\nabla}\cdot\vec{u}=0,\quad \vec{\nabla}\cdot\vec{B}=0. \tag{7}$$

Here Re is the Reynolds number, $\mathrm{Rm}=\mathrm{Re}\,\mathrm{Pr}_m$ is the magnetic Reynolds number, Pr_m is the magnetic Prandtl number. In the dissipationless limit Eqs. (7) conserve three quadratic integrals. In a three-dimensional case, these are the total energy E_t, the cross helicity H_C, and the magnetic helicity H_B,

$$E_t=\int\ (\vec{u}^2+\vec{B}^2)dV, \tag{8}$$

$$H_C=\int\ (\vec{u}\cdot\vec{B})dV, \tag{9}$$

$$H_B=\int\ (\vec{A}\cdot\vec{B})dV, \tag{10}$$

where $\vec{B}=\mathrm{rot}\vec{A}$. In two dimensions the latter integral is replaced by the square of vector potential $\vec{A}$:

$$a=\int\ (\vec{A}\cdot\vec{A})dV. \tag{11}$$

It should be noted that the hydrodynamic helicity

$$H_V=\int\ (\vec{u}\cdot\mathrm{rot}\vec{u})dV \tag{12}$$

is conserved only if $\vec{B}\to\vec{0}$, i.e., in a kinematic problem. In the kinematic limit the model also conserves a quantity analogous to H_V.

Let us introduce now the shell model in the form

$$(d_t+\mathrm{Re}^{-1}k_n^2)U_n=ik_n\Big\{(U_{n+1}^*U_{n+2}^*-B_{n+1}^*B_{n+2}^*)$$
$$-\frac{\varepsilon}{2}(U_{n-1}^*U_{n+1}^*-B_{n-1}^*B_{n+1}^*)$$
$$-\frac{(1-\varepsilon)}{4}(U_{n-2}^*U_{n-1}^*-B_{n-2}^*B_{n-1}^*)\Big\}$$
$$+f_n. \tag{13}$$

$$(d_t+\mathrm{Re}_m^{-1}k_n^2)B_n$$
$$=ik_n\Big\{(1-\varepsilon-\varepsilon_m)(U_{n+1}^*B_{n+2}^*-B_{n+1}^*U_{n+2}^*)$$
$$+\frac{\varepsilon_m}{2}(U_{n-1}^*B_{n+1}^*-B_{n-1}^*U_{n+1}^*)$$
$$+\frac{(1-\varepsilon_m)}{4}(U_{n-2}^*B_{n-1}^*-B_{n-2}^*U_{n-1}^*)\Big\}+g_n. \tag{14}$$

If $B_n=0$, one again obtains GOY equation (1). Equations (13) and (14) conserve the total energy E_t and the cross helicity H_C for any ε_m. The value ε_m is determined from the requirement of conservation of a sum, which corresponds to the third integral. For 3D this sum is

$$H_B=\sum_n\ (-1)^n k_n^{-1}|B_n|^2, \tag{15}$$

which is conserved, if only $\varepsilon=1/2$ and $\varepsilon_m=1/3$. For 2D the sum is

$$a=\sum_n\ k_n^{-2}|B_n|^2, \tag{16}$$

which gives $\varepsilon=5/4$ and $\varepsilon_m=-1/3$.

Let us note that ε and ε_m are the only parameters in our model, which are connected with the dimension of the MHD problem under consideration. However, it is not obvious that the choice $\varepsilon=5/4$, $\varepsilon_m=-1/3$ inevitably results in a magnetic field decay. Later we will demonstrate that this fact is really true for our model.

Recall that the problem of turbulent dynamo is not restricted to 2D and 3D situations, only. Zeldovich [26] treated a problem of 3D magnetic field enhancement in 2D hydrodynamic flow. However, possibilities of GOY models are too limited to choose ε and ε_m in such a way as to conserve 2D quantities for hydrodynamic variables and 3D ones for magnetic variables.

The terms f_n and g_n correspond to hydrodynamic and magnetic forcing, respectively. The first one is commonly used in dynamo theory, though one can also consider a free-decaying turbulence with a magnetic field generation. This approach can be a reasonable approximation, because the hydromagnetic decay time can be much larger than the time of magnetic field growth. As for the term g_n, its value is related to the very essence of dynamo mechanism, suggesting the magnetic field generation without external currents as magnetic field sources. Therefore, in the dynamo theory it is normally assumed that $g_n=0$. However, looking for the spectral properties of small-scale MHD turbulence, one can use this term to describe the action of the large-scale mag-

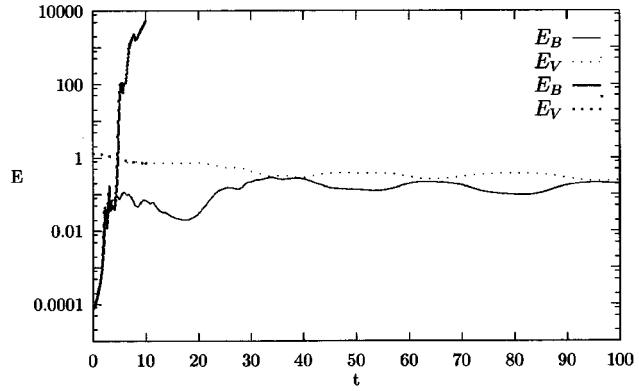

FIG. 1. Free decaying 3D MHD turbulence: kinetic E_V and magnetic E_B energy vs time in nonlinear (thin lines) and linear (thick lines) cases. Here and below all the variables in figures are given in dimensionless units.

netic field. We shall do this in Sec. III B in the context of the stationary forced MHD turbulence.

C. Numerical implementation

A number of numerical experiments was performed in the framework of models under discussion. The number of shells used in the simulations was typically of the order of $30(-4\leqslant n\leqslant 27)$. The system was forced near the zero shell $(n=0)$.

The time integration has been done using the fourth-order Runge-Kutta method with fixed time step. We tried also the ''slaved leap frog'' method, which gives the same results with comparable efficiency. The typical time step was 2.5×10^{-6}.

In shell models, each scale is described by only one mode, without reference to any spatial distribution. Therefore, statistics can be obtained only as time-averaged characteristics. Runs up to 10^7 time steps appeared to be enough to get a distinct picture of the process under consideration.

In addition to the above-mentioned quantities, we compute the structure functions defined by

$$s_n(q)=\langle |z_n|^q\rangle, \tag{17}$$

where z_n is one of the shell variables U_n or B_n.

III. RESULTS

A. Magnetic energy evolution in free decaying turbulence

We consider here the shell model without any, even hydrodynamic, forcing. Of course, this turbulence will decay in the remote future followed by the decay of magnetic field. Thus, strictly speaking, we discuss here the transient states. However, the decay time scale of turbulence appears to be much longer than the time scale of the development of the steady-state magnetic field distribution.

The initial distribution of energy corresponds in all cases to $E_V(k)\sim E_B(k)\sim k^{-2}$ (for $n\geqslant 0$), but the level of magnetic energy spectrum has been taken essentially lower than the kinetic one ($E_V\sim 1$, $E_B\sim 0.0001E_V$). The Reynolds number was $\mathrm{Re}=10^7$, the magnetic Prandtl number $\mathrm{Pr}_m=10^{-3}$.

Figure 1 demonstrates the magnetic energy evolution in a 3D shell model. We see that very soon, in time of order 1 (i.e., l/v in dimensional units) the magnetic energy reaches a level of about 1/10 of kinetic energy. There appears a relative long period of nonlinear evolution (about 20 dimensionless time units), after which a steady state is achieved. Magnetic and kinetic energy are approximately equal, though the magnetic energy periodically takes slightly lower values. A very slow decay of turbulence due to viscosity and Ohmic losses is also visible.

Also shown in Fig. 1 is the corresponding kinematic result, where any backaction of magnetic field on the flow is neglected. Now, the magnetic field growth is unbounded. Let us note that the kinematic growth is rather more intermittent than continuous: from time to time the growth is interrupted by the periods of temporal decay. The temporal evolution during the nonlinear regime is much more regular.

These results are in general agreement with the available knowledge concerning 3D turbulent dynamo. However, some specific features should be mentioned. Direct computer simulations of a turbulent dynamo in terms of complete MHD equations usually demonstrate that the magnetic energy is several times lower than the kinetic one (see, e.g., [9]). We are inclined to identify this result with the first stage of the nonlinear evolution presented in Fig. 1. Because direct numerical simulations are extremely time consuming, it is very difficult to gain deep insight into nonlinear evolution. Our simulations support the concept that the turbulent dynamo gives an (intermittent) growth of magnetic field and magnetic energy, not only the growth of ensemble averaging magnetic energy (see, e.g., [8]). Let us note that this conclusion is not always valid. Indeed, the equation

$$\frac{\partial \phi}{\partial t}=U\phi+\nu\Delta\phi \tag{18}$$

in the unbounded space, where U is a short-correlated random function with vanishing mean value, demonstrates an exponential growth of the ensemble averaged energy $\langle\phi^2\rangle$ and a simultaneous decay of each realization of random field ϕ with probability 1. In other words, a growth of ensemble average $\langle\phi^2\rangle$ for Eq. (18) appears only as a result of exponentially rare realizations of U [8]. Since the analysis of the Kazantsev equation gives information concerning the averaged values of $\langle H^2\rangle$, one needs an additional treatment of typical realization.

The results of numerical simulation for the 2D case are presented in Fig. 2. The magnetic energy for nonlinear, as well as kinematic, cases are slowly decaying in time. This decay is, however, intermittent and the intermittency is much more pronounced in the kinematic case. We note that the magnetic energy decay in the 2D case has the time scale much longer than l/v. To clarify this fact, we present also the spectral distribution of kinetic E_V and magnetic E_B energy in different stages of evolution (for the 2D case see Figs. 3 and 4). It is remarkable that the magnetic energy, being much less than the kinetic one (Fig. 2), is in equipartition with the kinetic energy in some wavelength range, which corresponds to relatively small scales, preceding the dissipative ones ($n\approx 6-8$ in Fig. 3). The magnetic energy decay in this range occurs with the same rate as that of energy. This persistence of turbulent magnetic field could not be treated in Zeldov-

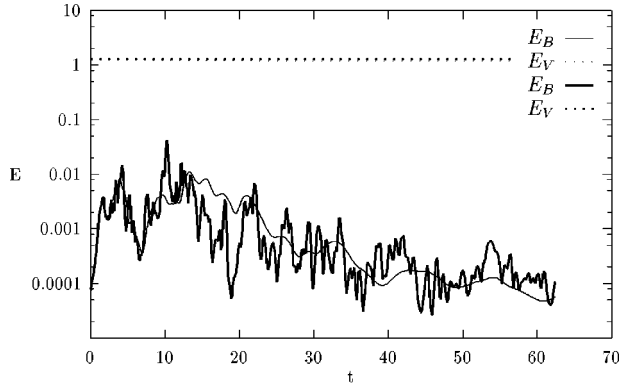

FIG. 2. Free decaying 2D MHD turbulence: kinetic E_V and magnetic E_B energy vs time in nonlinear (thin lines) and linear (thick lines) cases.

ich's [26] analysis. The kinetic energy keeps almost the same value during the whole time of evolution in both cases (Fig. 2), while in 2D a stable level of the total kinetic energy reflects only the fact of energy condensation in the large scales, where the influence of the magnetic field is negligible. However, the situation in the small scales is quite different (compare Fig. 3 and Fig. 4): in the nonlinear case, the small-scale kinetic energy becomes accessible to the dynamo mechanism and is involved in its action, so the spectrum $E_V(k)\sim k^{-3}$ is established at a later stage of evolution for all $n\geqslant 0$. In the linear case, the initial distribution of kinetic energy [$E_V(k)\sim k^{-2}$, which is a slow decay for 2D] leads to a typical two-dimensional scenario of the spectrum evolution with an inverse energy transfer and a direct enstrophy transfer. As a result, the energy in large-scale shells (up to n about 5) for $t=30$ becomes higher than for $t=0$, and only for $n>5$ is there an interval of the enstrophy transfer with the spectrum like k^{-3} (see Fig. 4).

Let us note that the points in the figures indicate the energy of a shell, i.e., the energy of the whole octave of wave numbers. Therefore, if the energy spectrum is governed by the power law $E(k)\sim k^{-\alpha}$, the shell energy distribution gives the slope, which is different by a unit, i.e., $E(n)\sim k_n^{1-\alpha}$. So, the well pronounced power behavior of magnetic energy E_B in the intermediate scales ($0\leqslant n\leqslant 8$) at later time of the 2D linear decay (Fig. 4) gives $E_B(n)\sim k_n$ and corresponds to $E_B(k)\sim k^0\sim$ const.

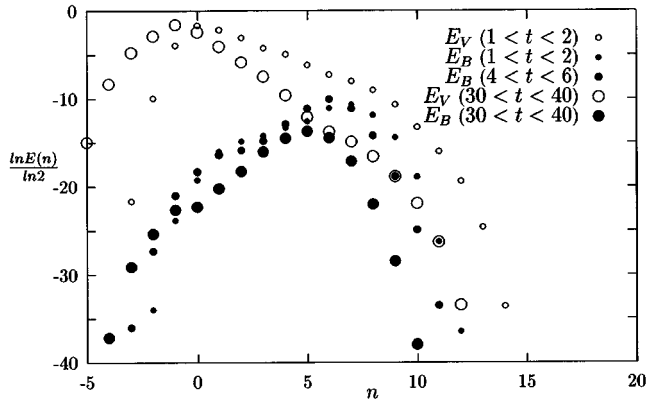

FIG. 3. Free decaying 2D MHD turbulence (nonlinear case): evolution of spectra of kinetic E_V and magnetic E_B energy.

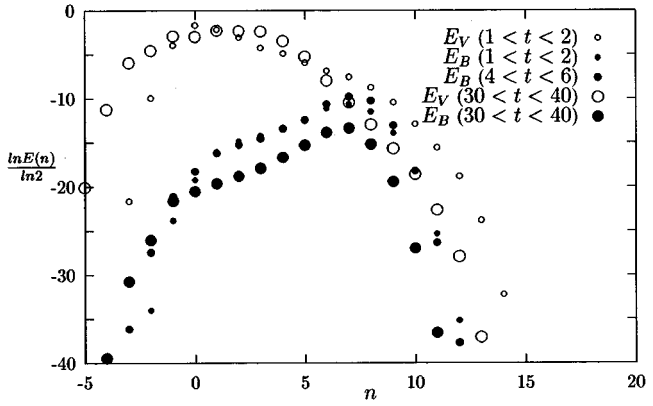

FIG. 4. Free decaying 2D MHD turbulence (linear case): evolution of spectra of kinetic E_V and magnetic E_B energy.

Figures 5 and 6 present the spectra for the 3D case. In the linear case (Fig. 6) the spectra show that the infinite growth of magnetic energy occurs at an intermediate range of scales, limited by dissipation at higher wave numbers.

The spectra for 3D nonlinear force-free evolution are given in Fig. 5. It can be readily seen that there is no unified spectral slope for the magnetic and the kinetic energy. The spectral slope for the kinetic energy is very similar to Kolmogorov's ''$-5/3$'' law (shown in Fig. 5 by solid line), and the magnetic spectrum for the range of large k is evidently steeper (something like k^{-2}). It is quite obvious that both are steeper than Kraichnan-Iroshnikov's ''$-3/2$'' law.

One can also note that at the early stage of evolution, when the magnetic energy remains significantly lower than the kinetic one, the magnetic energy shows the distribution like $E_B(k)\sim k^{-1}$ [in Figs. 5 and 6 $E_B(n)\sim$ const for $2\leqslant n\leqslant 6$]. This spectrum is discussed by Ruzmaikin and Shukurov [11].

For the range of moderate k both 2D and 3D models give growing power law magnetic spectra, typical for analytical theories of small-scale dynamo. However, in agreement with analytical predictions, this range is more pronounced in the 2D model (we are grateful to D. Biskamp, who attracted our attention to this fact).

To clarify the spectral index problem we consider the sta-

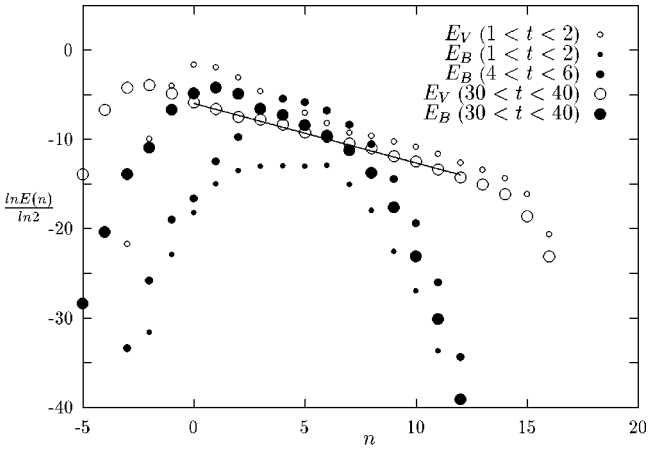

FIG. 5. Free decaying 3D MHD turbulence (nonlinear case): evolution of spectra of kinetic E_V and magnetic E_B energy.

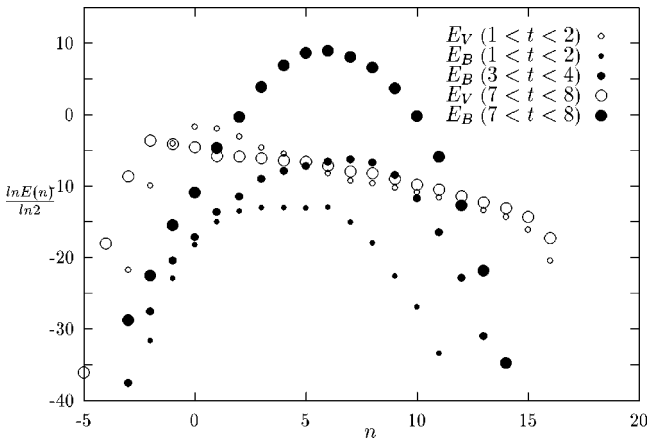

FIG. 6. Free decaying 3D MHD turbulence (linear case): evolution of spectra of kinetic E_V and magnetic E_B energy.

tionary forced MHD turbulence. The results of this study are presented in the next section.

B. Spectral index in stationary forced MHD turbulence

The turbulent magnetic field, produced by the small-scale dynamo, does not possess a noticeable magnetic helicity H_B. On the other hand, generation of small-scale magnetic field due to a turbulent decay of the large-scale magnetic field creates the small-scale helical magnetic field. Indeed, the total magnetic field can be presented as $\mathbf{H}=\mathbf{B}+\mathbf{b}$, where $\mathbf{B}$ is the large-scale magnetic field and $\mathbf{b}$ the small-scale one. In contrast to magnetic helicity of the field $\mathbf{H}$, which obeys the conservation law, the magnetic helicity of the large-scale field $\mathbf{B}$ is not a conserved quantity, because its diffusion is governed by the *turbulent* diffusivity. Since the turbulent diffusivity is not negligible, the large-scale magnetic field $\mathbf{B}$ is not frozen into the flow. Hence, we conclude that it is necessary to introduce the magnetic helicity into the small scales to compensate the growing helicity of the large-scale magnetic field. This helicity, as well as the other effects of large-scale magnetic field, should be described in our model through the magnetic force g_n, because our shell model has no quantities responsible for the large-scale magnetic field.

We simulate the Equations (13) and (14) for different initial conditions and forces f_n and g_n. Now $\mathrm{Re}=10^{10}$, $\mathrm{Pr}_m=1$. We start with the situation corresponding to 3D MHD turbulence ($\epsilon=0.5$, $\epsilon_m=0.33$) and consider the stationary forced hydrodynamic turbulence [the magnetic force $g_n=0$ and the kinematic force acting only in the zero shell: $f_0=0.002(1+i)$]. For $t=0$ a seed magnetic field has been introduced as a weak white noise. The stationary spectra obtained by time averaging over the interval $5<t<25$ are presented in Fig. 7, showing a Kolmogorov-type spectral distribution with a slow but stable dominance of magnetic energy in the whole inertial range. The total values of energy ($E_V=1.1$, $E_B=0.7$) reflect only the relatively low level of magnetic energy in the largest scales (for $n<2$). The spectral flux of energy is shown in the lower panel of Fig. 7. We plot separately the flux of kinetic energy, the flux of magnetic energy, and their sum, called the total flux. The latter is approximately constant for $2<n<20$ and supports the fact that a state with well developed cascade transfer of energy

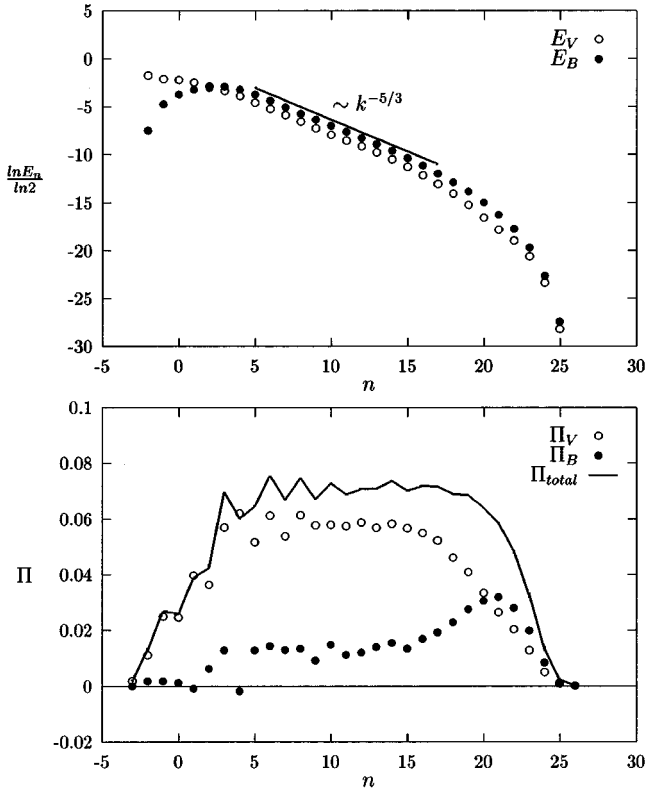

FIG. 7. Energy spectra and fluxes in stationary forced 3D MHD turbulence. Only the mechanical force f_n is active ($g_n=0$).

has been established. Although the magnetic energy is larger than the kinetic one, the kinetic flux evidently dominates in all scales up to the dissipative ones. It should be emphasized that the steady-state value of cross helicity is low ($H_C\sim0.05$), as well as the level of magnetic helicity, which is $H_B\sim0.001$. It is remarkable that the magnetic energy flux is relatively large, and is much larger than the kinematic one at the small scale range.

Now, we consider a simultaneous kinetic and magnetic forcing in the same scales by changing the initial value of cross helicity H_C and magnetic helicity H_B and controlling the input of both quantities by the external forces.

If both H_C and H_B remain much less than the energy, the stationary state is quite similar to that of pure mechanical forcing. The only difference is that the large-scale range of the magnetic energy spectrum becomes more similar to the kinetic one. The results do not change, if the initial distribution of the variables B_n and the forces f_n and g_n provide the highest level of magnetic helicity $H_B\sim E_B$, and a low level of cross helicity. This case is presented in Fig. 8, where for $5<n<15$ the spectrum is fitted by $E(k)\sim k^{-1.69\pm0.02}$.

The Kolmogorov-type spectra also appear in the corresponding 2D case (Fig. 9). Let us note that in pure hydrodynamic 2D turbulence the Kolmogorov's inertial range with direct cascade of energy does not appear due to the enstrophy conservation. However, the magnetic field violates this conservation law, and a direct cascade with corresponding production of enstrophy is expected for 2D MHD turbulence [19].

An unexpected result has been obtained for the case, shown in Fig. 10. The simultaneous input of large-scale cross

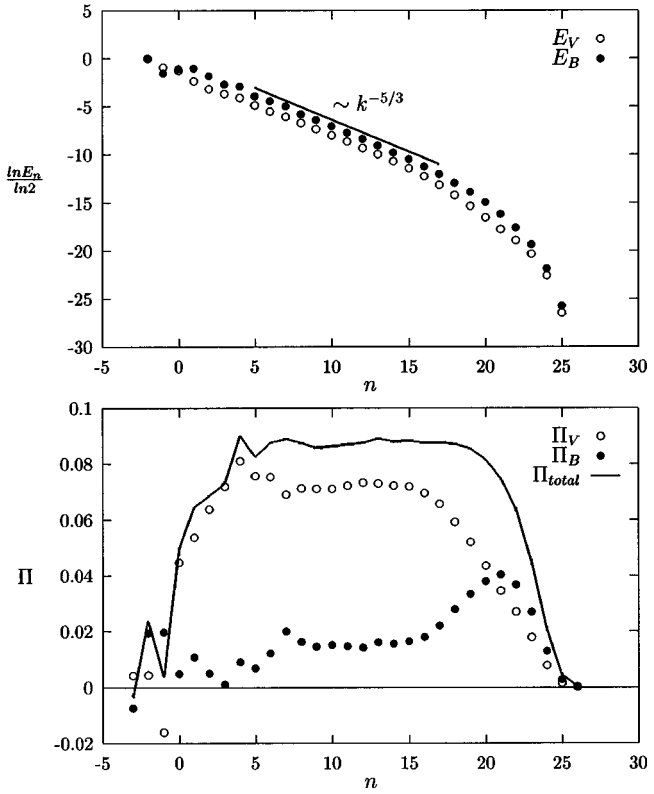

FIG. 8. Energy spectra and fluxes in stationary forced 3D MHD turbulence. The mechanical and the magnetic forces provide equal inputs of energy in the shell with number $n=0$ ($f_0=g_0$). The inputs of H_B and H_C are controlled by the values of f_{-1} and g_{-1}. Here the magnetic helicity is strong and the cross helicity is week ($H_B \sim E_B \sim E_U$, $H_C \sim 0$).

and magnetic helicities completely destroys the cascade process. No inertial range with a constant spectral flux of energy is visible. Let us emphasize that the energy flux in Fig. 10 is an order of magnitude lower than in other figures. The slope of the spectrum becomes very steep and gives for the same range of scales $5<n<15$ the value -1.90 ± 0.04.

A state with a spectral distribution like the Kraichnan-Iroshnikov solution with the spectral index ''$-3/2$'' appears only in the case when the forcing provides vanishing magnetic helicity, the cross helicity being of the same order of magnitude as the energy (Fig. 11). Though the spectrum presented on this plot is complicated, a power law range with index ''$-3/2$'' seems to be visible and a relatively constant energy flux is present.

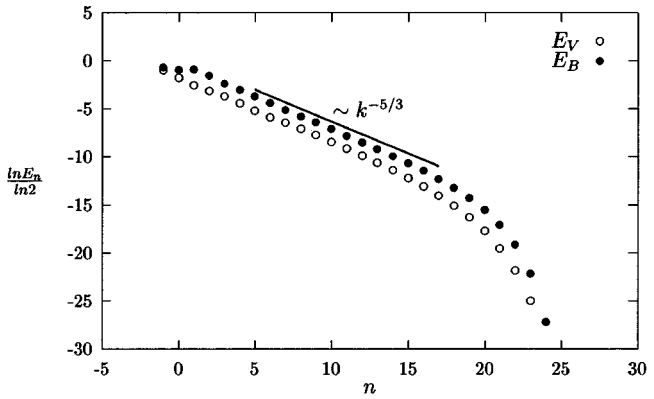

FIG. 9. Energy spectra in stationary forced two-dimensional MHD turbulence ($H_C \sim 0$).

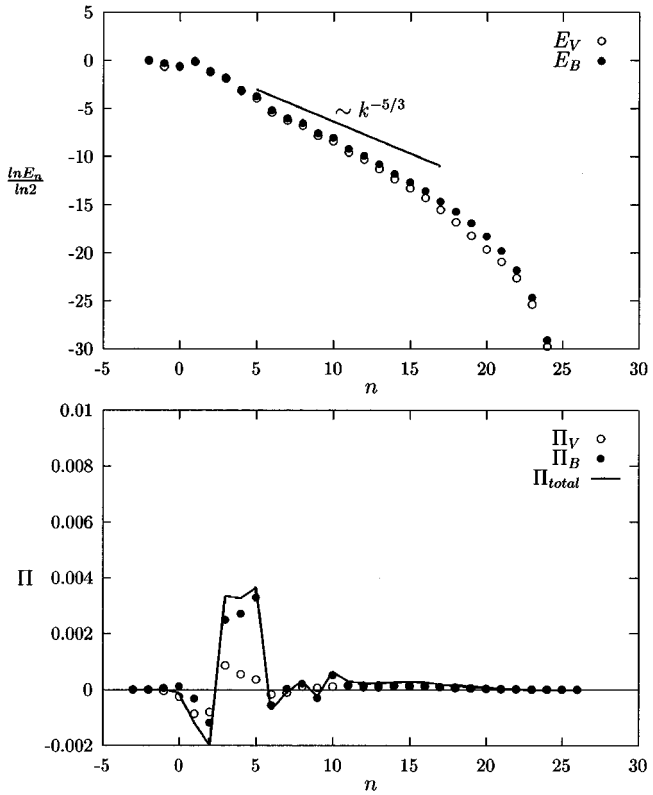

FIG. 10. Energy spectra and fluxes in stationary forced 3D MHD turbulence. Here both cross-helicity magnetic helicity are large ($H_C \sim E_u \sim E_B$, $H_B \sim E_B$).

IV. DISCUSSION

Our shell model of MHD turbulence is evidently a drastic simplification of the detailed spatial-temporal picture of MHD turbulence governed by the Navier-Stokes and Maxwell equations. However, the performed analyses demonstrate that the model correctly reproduces the bulk of information on the small-scale dynamo known from the previous studies of the Kazantsev equation, as well as from numerics. A small-scale dynamo can be investigated to some extent by direct asymptotic analysis of the explicit solution of induction equation in terms of Wiener functional integrals [33]. This direct method supports the results known from the analytical studies of the Kazantsev equation. However, their applications are restricted by the following fact.

There is an analogy between magnetic field behavior in 2D turbulent flow and temporal amplification of temperature gradients in a turbulent flow [26]. Obviously, temperature differences in a turbulent flow can only decrease with time provided no external heating is available. However, temperature gradients in 3D, as well as in 2D turbulence, are temporary, growing due to a mixing of hot and cold fluid particles. This analogy is not applicable to the magnetic field in 3D turbulence, where the small-scale dynamo is active and magnetic field in a kinematic approximation has an infinite rather than a temporal growth. This fine difference is a well-known problem in verification of direct analytical investigation of

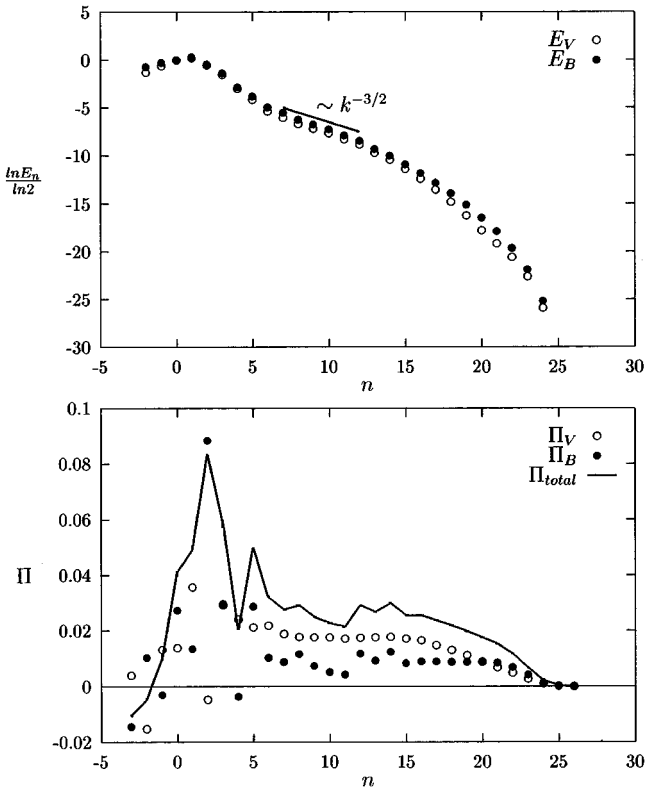

FIG. 11. Energy spectra and fluxes in stationary forced 3D MHD turbulence with a high level of cross helicity and a low level of magnetic helicity ($H_C \sim E_u \sim E_B$, $H_B \sim 0$).

the induction equation in a turbulent flow and to some extent of the Kazantsev equation, because it is a challenging task to follow in the above analysis (see the discussion in [33]).

However, the shell models are free of this problem. To verify this fact, we consider a shell model for temperature evolution in a turbulent flow, which uses the same GOY equation for the velocity pulsations and the corresponding equation for the temperature variables T_n, which conserves in a diffusionless limit only one quadratic quantity $E_T = \Sigma T_n^2$:

$$[d_t + (\mathrm{Re})^{-1} k_n^2] U_n = i k_n \left\{ U^*_{n+1} U^*_{n+2} - \frac{\varepsilon}{2} U^*_{n-1} U^*_{n+1} - \frac{(1-\varepsilon)}{4} U^*_{n-2} U^*_{n-1} \right\}, \tag{19}$$

$$(d_t + (\mathrm{Re\ Pr})^{-1} k_n^2) T_n = i k_n \left\{ (U^*_{n+1} T^*_{n+2} + T^*_{n+1} U^*_{n+2}) + \frac{1}{2} (U^*_{n-1} T^*_{n+1} + T^*_{n-1} U^*_{n+1}) - \frac{1}{4} (U^*_{n-2} T^*_{n-1} + T^*_{n-2} U^*_{n-1}) \right\}. \tag{20}$$

We have analyzed the force-free decay described by Eqs. (19) and (20) for the same initial conditions as for MHD turbulence. For thermal energy the time behavior in 2D and 3D is very similar. The evolution of the thermal energy and temperature gradients is shown in Fig. 12 for 3D cases. As might be expected, the thermal energy is a smoothly decaying quantity, while the temperature gradients exhibit a temporal growth followed by a decay.

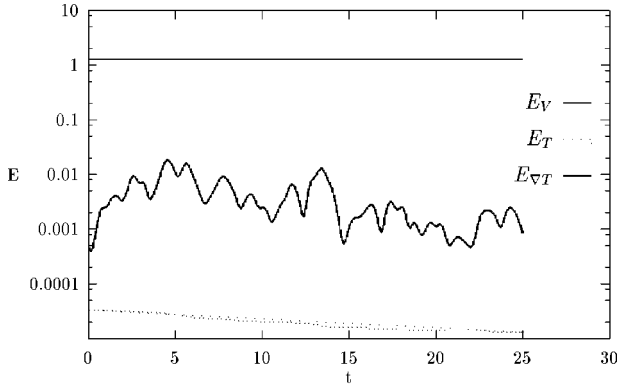

FIG. 12. Free decaying 3D turbulence with passive scalar (temperature): the kinetic energy E_V, the energy of temperature pulsations E_T, and the mean square of gradients of temperature $E_{\nabla T}$ vs time.

Now we can summarize with more confidence the result obtained by our shell model, which could hardly be verified in analytical or numerical studies of small scale dynamo.

(1) The transition from kinematic dynamo to equilibrium magnetic field distribution appears to be a relatively long process lasting a dozen turnover times. At this stage, magnetic energy grows by about an order of magnitude.

(2) In the kinematic, as well as in the nonlinear approximation, the magnetic field decay in 2D turbulence is a very slow process. It takes many dozens of turnover times and involves many stages of temporal magnetic field amplifications.

(3) An existence of large-scale magnetic field can essentially modify the properties of small-scale fields generated by a turbulent flow. The latter strongly depend on the cross helicity and the magnetic helicity generated by the large-scale MHD flow and introduced by it in the small scales. As the cross helicity is a kind of measure of correlations between the velocity and the magnetic fields, our results mean that if U and B are not correlated (at least H_C is close to 0) one gets the Kolmogorov-type solution with spectra close to the ''$-5/3$'' law. This state is independent of the level of the magnetic helicity H_B.

(4) If the magnetic and velocity fields are correlated, the Kolmogorov state is not established. Then the result depends on the magnetic helicity.

(5) The high level of H_B suppresses any cascade of energy. The spectral energy flux decreases and the spectra become steep. This occurs when the velocity and magnetic fields are correlated and the magnetic helicity is negligible. In this case, an Iroshnikov-Kraichnan-type state is established. Let us emphasize once more that our result is very different from the result of Biskamp, who has obtained the Iroshnikov-Kraichnan state in a shell model by introducing an additional interaction of any shell with the shell, which describes the largest scale of magnetic field. His model directly followed the basic idea that the Iroshnikov-Kraichnan state appears as a result of direct interactions of the velocity

TABLE I. Scale exponents ζ_q for the structure functions of different order q.

q	ζ_q				
	$K41$	HD experimend [34]	HD shell model [32]	MHD shell model U	B
1	1/3		0.40	0.34 ± 0.01	0.33 ± 0.01
2	2/3	0.71	0.71	0.66 ± 0.02	0.64 ± 0.02
3	1	1	1.02	0.94 ± 0.03	0.91 ± 0.04
4	4/3	1.28	1.27	1.20 ± 0.04	1.17 ± 0.06
5	5/3	1.53	1.53	1.45 ± 0.07	1.40 ± 0.10
6	2	1.78	1.81	1.65 ± 0.10	1.62 ± 0.14

pulsations δv_l and magnetic pulsations δB_l of given scale l with the large-scale magnetic field. In our case the model includes only the local interactions and the effect of the large-scale magnetic field is provided only by the input flux of the quadratic quantities, conserved by the MHD turbulence.

In our numerical experiments we have also checked the behavior of higher structure functions, which should reflect the level of intermittency of the cascade processes. However, it should be emphasized that one can consider only the time intermittency in a system like shell models, and that the most unexpected result, obtained by the shell models, was that they reproduce with a good accuracy the behavior of the structure functions in a real hydrodynamic turbulence.

To compare the pure hydrodynamic Kolmogorov state and the magnetohydrodynamic Kolmogorov-type state (we study the case when only the kinetic energy is introduced in the system, for which the spectra are shown in Fig. 7) we present in Table I the scale exponents ζ_q for the structure functions of order q, which are defined by

$$S_q(l)\sim l^{\zeta_q}. \tag{21}$$

Given in the table are the six lower-scale exponents. The first column gives the order number q, the second one shows the classical 1949-year Kolmogorov dimensional prediction for the scale exponents (following the linear law $\zeta_q=q/3$). The third column shows the experimental values for a turbulent flow given in [34], the next one presents the values obtained by the hydrodynamic GOY shell model [32]. These two columns demonstrate that the values given by the shell model are not far from the experimental values. The two last columns give the scale exponents, calculated by our MHD shell model in the case when the system was forced only by the ''mechanical'' force f_0 and has a ''$-5/3$'' spectral distribution.

Two conclusions can be drawn from the data in the table. First of all, regardless of the shape of the spectra, which display a well pronounced ''$-5/3$'' law, the state of the system does not correspond to the Kolmogorov turbulence. Let us recall that for hydrodynamical turbulence $\zeta_3=1$, which proves to be untrue in the MHD state. Secondly, the level of intermittency in MHD turbulence is higher than in the hydrodynamic case and the level of intermittency for the magnetic field is slightly higher than in the velocity field.

To conclude, let us emphasize once more that the shell models reproducing correctly many features of turbulent flows are a drastic simplification of fluid motion equations. In particular, they ignore any information on the spatial structure of motion and involve only the spatial dimension through the conservation laws. This fact is especially impressive in the magnetohydrodynamic turbulence, where the main understanding of physical processes resulting in magnetic field generation is gained from the topological analysis of magnetic tubes net.

From the viewpoint of the shell model theory the only difference between 2D and 3D shell models is the different choice of the model coefficients. By restricting ourselves to the shell model theory, it is difficult to motivate why the choice $\epsilon=5/4$, $\epsilon_m=-1/3$ leads to magnetic field decay.

Two explanations of this fact can be proposed. Either is possible to avoid the topological arguments in explanation of the difference between the 2D and 3D flows, or to identify topological features of the flow in the coefficients of the shell model.

ACKNOWLEDGMENTS

Financial support from the Russian Foundation of Basic Research (under Grant No. 96-02-16252-a) is kindly acknowledged. P.F. thanks the Center for Parallel Computers of Royal Institute of Technology (Stockholm) for hospitality. We are grateful to L. V. Semukhina for assistance in improving the text.

[1] H. K. Moffatt, *Magnetic Field Generation in Electrically Conducting Fluids* (Cambridge University Press, Cambridge, 1978).
[2] G. K. Batchelor, Proc. R. Soc. London, Ser. A **261**, 405 (1950).
[3] A. P. Kazantsev, Sov. Phys. JETP **26**, 1031 (1968).
[4] R. H. Kraichnan and S. Nagarajan, Phys. Fluids **10**, 859 (1967).
[5] S. I. Vainstein, Zh. Eksp. Teor. Fiz. **58**, 153 (1970) [Sov. Phys. JETP **31**, 87 (1970)].
[6] S. I. Vainstein, Zh. Eksp. Teor. Fiz. **83**, 161 (1988) [Sov. Phys. JETP **56**, 86 (1982)].
[7] V. G. Novikov, A. A. Ruzmaikin, and D. D. Sokoloff, Zh. Eksp. Teor. Fiz. **85**, 909 (1983) [Sov. Phys. JETP **58**, 527 (1983)].
[8] Ya. B. Zeldovich, S. A. Molchanov, A. A. Ruzmaikin, and D. D. Sokoloff, Sov. Sci. Rev. Math. Phys. **7**, 1 (1988).
[9] M. Meneguzzi, U. Frisch, and A. P. Pouquet, Phys. Rev. Lett. **47**, 1060 (1981).
[10] A. P. Kazantsev, A. A. Ruzmaikin, and D. D. Sokoloff, Zh. Eksp. Teor. Fiz. **88**, 487 (1985) [Sov. Phys. JETP **61**, 285 (1985)].
[11] A. A. Ruzmaikin and A. M. Shukurov, Astrophys. Space Sci. **82**, 397 (1982).
[12] R. M. Kulsrud and S. W. Anderson, Astrophys. J. **396**, 606 (1992).

[13] R. S. Iroshnikov, Sov. Astron. **40**, 742 (1963).
[14] R. H. Kraichnan, Phys. Fluids **8**, 1385 (1965).
[15] A. A. Ruzmaikin, P. C. Liewer, and J. Feynman, Geophys. Astrophys. Fluid Dyn. **73**, 163 (1993).
[16] A. D. Poezd and D. D. Sokoloff, Astron. Rep. **31**, 197 (1993).
[17] J. M. Finn and E. Ott, Phys. Rev. Lett. **60**, 760 (1988).
[18] S. Childress and A. D. Gilbert, *Stretch, Twist, Fold: The Fast Dynamo* (Springer, Berlin, 1995).
[19] P. Frick, Magn. Gidrodin. **1**, 60 (1983) [Magnetohydrodynamics **20**, 262 (1984).
[20] C. Gloaguen, J. Leorat, A. Pouquet, and R. Grappin, Physica D **17**, 154 (1985).
[21] R. Grappin, J. Leorat, and A. Pouquet, J. Phys. (France) **47**, 1127 (1986).
[22] V. Carbone, Phys. Rev. E **50**, 671 (1994); Europhys. Lett. **27**, 581 (1994).
[23] A. Brandenburg, K. Enquist, and P. Olesen, Phys. Rev. D **54**, 1291 (1996).
[24] D. Biskamp, Phys. Rev. E **50**, 2702 (1994).
[25] L. Kadanoff, D. Lohse, J. Wang, and R. Benzi, Phys. Fluids **7**, 617 (1995).
[26] Ya. B. Zeldovich, Zh. Eksp. Teor. Fiz. **31**, 154 (1956) [Sov. Phys. JETP **4**, 460 (1957)].
[27] Ya. B. Zeldovich, A. A. Ruzmaikin, S. A. Molchanov, and D. D. Sokoloff, J. Fluid Mech. **144**, 1 (1984).
[28] E. B. Gledzer, Dokl. Akad. Nauk. SSSR **209**, 1046 (1973) [Sov. Phys. Dokl. **18**, 216 (1973)].
[29] V. N. Desnjansky and E. A. Novikov, J. Appl. Math. Mech. **38**, 468 (1974).
[30] L. Biferale, A. Lambert, R. Lima, and G. Paladin, Physica D **80**, 105 (1995).
[31] M. Yamada and K. Ohkitani, J. Phys. Soc. Jpn. **56**, 4210 (1987).
[32] P. Frick, B. Dubrulle, and A. Babiano, Phys. Rev. E **51**, 5582 (1995).
[33] S. A. Molchanov, A. A. Ruzmaikin, and D. D. Sokoloff, Geophys. Astrophys. Fluid Dyn. **30**, 241 (1984).
[34] R. Benzi, S. Ciliberto, C. Baudet, F. Massaioli, R. Tripiccione, and S. Succi, Phys. Rev. E **48**, 29 (1993).